JOURNAL OF GEOPHYSICAL RESEARCH, VOL. 103, NO. B9, PAGES 21,059–21,065, SEPTEMBER 10, 1998

Duration of deep earthquakes determined by stacking of Global Seismograph Network seismograms

A. G. Bos
Department of Earth Sciences, Utrecht University, Utrecht, Netherlands

G. Nolet and A. Rubin
Department of Geosciences, Princeton University, Princeton, New Jersey

H. Houston and J.E. Vidale
Earth and Space Sciences Department, University of California, Los Angeles

Abstract. The duration of each subevent of 48 earthquakes with magnitude larger than 5.5 and depth greater than 100 km was determined from stacked traces of broadband records of Global Seismograph Network stations. We fitted the source time function by one or more triangles convolved with attenuation. We found that global stacks of displacement seismograms yield reliable estimates of the rupture duration. The durations, scaled to a moment of 10^{19} N m, of both the subevents and the entire earthquake show a slight decrease with depth from 9 s for events at 100 km depth to about 7 s for events at 600 km depth. Assuming that the rupture velocity is a constant fraction of the shear wave speed, this decrease can be completely explained by the increase in shear velocity of 20%. In this sense, deep earthquakes are comparable to intermediate ones. For some intermediate-depth events, *Vidale and Houston* [1993] found durations up to twice as long. We find that almost all of their slow events have been recorded at large epicentral distances. At these distances, we conjecture that the end of the P wave train may be extended by the arrival of reflections from the D" layer.

1. Introduction

Earthquake duration is an important characteristic of the rupture process. Whereas shallow earthquakes can be explained by a process involving simple failure or slip on a frictional surface, the mode of stress release at depths where the overburden pressure is too large to allow for simple frictional sliding is still a matter of much debate. Because of its dependence upon important characteristics of the rupture such as fault size, stress drop, and rupture velocity, earthquake duration is a potentially powerful, if somewhat imprecise, descriminant between mechanical models of deep earthquakes.

Not surprisingly therefore, the duration of earthquakes as a function of depth has been the subject of various observational studies. Modeling global broadband records, *Fukao and Kikuchi* [1987] and *Chung and Kanamori* [1980] found average values for deep events of about 8 and 7.5 s, respectively (scaled to a moment of 10^{19} N m). For events at intermediate depths, *Kanamori and Given* [1981], *Fukao and Kikuchi* [1987], *Ekström and Engdahl* [1989], and *Chung and Kanamori* [1980] all found scaled durations of about 10 s. This difference between the duration of deep and intermediate events is small enough to be explainable by the increase in shear velocity, and consequently the increase in rupture velocity, with depth. These results have not gone unchallenged though. By stacking short-period data from the western United States, *Vidale and Houston* [1993], hereafter called VH, found an average value of 11 s at 100 km depth with several very long-scaled durations at depths shallower than 300 km and found a significantly shorter average duration (5.5 s) for deep events. This represents roughly a halving of the duration time with depth which is far larger than may be attributed to the increase in shear velocity. It would imply a deviation from the scaling law known for shallow earthquakes and would therefore be a strong observational indication that the rupture process of deep earthquakes is fundamentally different from that of shallow ones.

Because of the important implications of the result of VH for the mechanics of deep earthquakes and the apparent discrepancy between theirs and the other studies, we undertook a new study for deep events by stack-

Paper number 98JB01352.
0148-0227/98/98JB-01352$09.00

ing broad-band recordings of the Global Seismograph Network (GSN). We expect an improvement in the determination of rupture duration not only because of the superior quality of the stations in the GSN network. We have also applied a new philosophy of global stacking rather than local stacking. In contrast to stacks over local networks, global stacks reduce the effects of scattering near the source and along the path since the rays leave the source in widely different directions and cross different regions inside the Earth. Global stacking allows us also to include events for which the local array is in the shadow zone or near a node in the radiation pattern. Finally, we make an additional distinction in this paper between the duration of the total rupture and the duration of individual subevents and analyze the depth dependence for both.

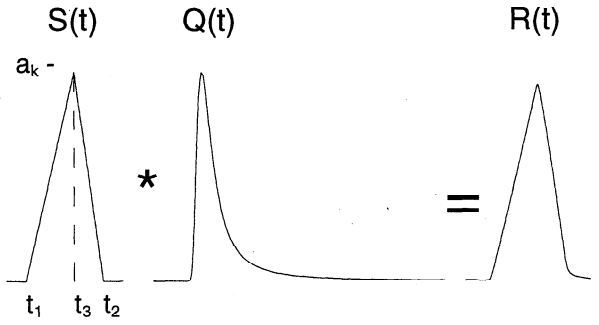

Figure 2. Construction of a triangular source time function. $S(t)$ represents the unattenuated triangle, $Q(t)$ is the attenuation factor of *Azimi et al.* [1968] and $R(t)$ is the result of the convolution. For clarity, the duration of $Q(t)$ is expanded (from a true duration of about 0.4 s).

2. Data Analysis

For this study we collected the Global Seismograph Network recordings of 48 strong ($M > 5.5$) and deep (> 100 km) events that occurred between May 1991 and September 1996. The somewhat uneven distribution of these events is shown in Figure 1. In this period the network recorded between 30 and 100 broadband vertical-component recordings per event. The magnitude range ensures that there is either sufficient duration of rupture or amplitude to measure reliably, whereas the depth range avoids the interference of surface reflected waves (pP and sP in the P wave train).

These teleseismic recordings have visibly coherent P waveforms. However, the crustal structure, which is different for each station, results in a tail of scattered waves following the direct P wave that distorts and obscures the later part of this arrival, and stacking is needed to obtain a good signal/noise ratio for the original P waveforms [*Vidale and Houston*, 1993]

We rejected seismograms that show a high noise level before the arrival of the P wave or seismograms in which the arrival of the PcP wave came within 10 s of the P wave arrival, as this arrival might interfere with the P wave and thus influence the duration measurement.

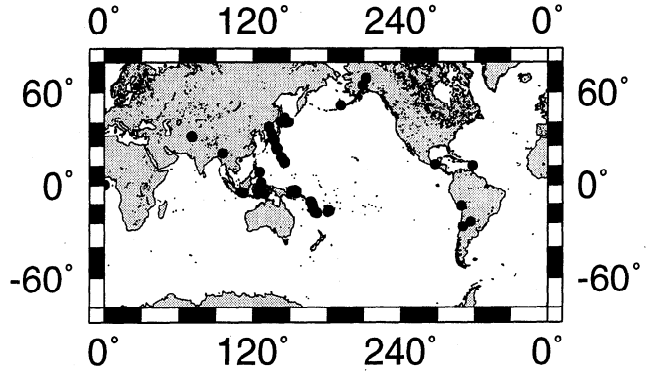

Figure 1. Locations of the events used in this study.

This leaves us with about 10-30 clean seismograms per event. The velocity traces are aligned using the cross-correlation of each trace with all others. For this we used the technique of *VanDecar and Crosson* [1990], modified to include a correction for polarity (which is not constant for a global stack) using the sign of the correlation coefficient. Estimating the noise level from a short time window before the P wave arrival, we scaled each seismogram to equalize the noise level before stacking.

Following VH, we assume that much of the scattered energy is incoherent between the stations; therefore noise is expected to diminish by a factor equal to the square root of the number of traces stacked. In this way we recover the source time function by canceling the scattered coda.

We integrated the stacks once to obtain the far-field displacement. This produces a very clear source pulse, sometimes consisting of several peaks. These peaks represent small subevents which together make up the event as recorded [*Frohlich* 1989; *Fukao and Kikuchi* 1987]. We model our source time function $S(t)$ as a sum of N subevents whose individual source time functions are given by triangular functions, $d_i(t)$, of duration τ, shifted in time

$$S(t) = \sum_{i=1}^{N} a_i d_i(t_1, t_2, t_3), \qquad (1)$$

where $d_i(t_1, t_2, t_3)$ is a triangle starting at t_1, ending at t_2 and peaking at t_3. The source duration τ is defined as $\tau = t_2 - t_1$ (Figure 2).

Of the 48 events, 22 showed clear indications that the rupture occurred not in one continuous failure of the fault plane but in the form of two or more subevents. For these, we measured the duration of subevents as well as the duration of the total rupture process, defined as the difference between the latest t_2 and the earliest t_1 among all subevents. Obviously, the total duration of rupture is a function both of the duration

of each subevent and of the separation in time of such subevents. Since the latter may convolute a simpler relationship between duration and, say, seismic moment, we expect, in principle, a cleaner scaling for subevents. This may be partly offset by the fact that the estimation of t_1 and t_2 for each subevent brings in an extra opportunity for measurement error.

Since the signal is attenuated by its path through the Earth, we convolve the triangles with an attenuation operator. We used the attenuation factor of *Azimi et al.* [1968], which avoids an infinite attenuation at small frequencies :

$$Q(\omega, m) = \exp(-m|\omega|^\gamma) \exp(im|\omega|^\gamma \tan\frac{\gamma\pi}{2}), \quad (2)$$

where $\omega \geq 0$ is the angular frequency measured in rad/s, $m = \beta_0 x$, β_0 is a constant representing the absorption properties of the medium, x is epicentral distance and $\gamma \sim 1$ is a dimensionless parameter that represents the almost linear relation of the absorption coefficient with the angular frequency. The effect of Q on the duration is small (about 0.4 s) and we disregard the even smaller variations to be expected between events above and below the asthenosphere. We used trial and error on a few records to determine appropriate values of Azimi's parameters that allow for good fits to the data. Using MKS units, we obtained values of $\beta_0 = 5 \times 10^{-7}$ and $\gamma = 0.90$, which were then fixed for all events. We fit the signal with the 'attenuated triangles' by minimizing the misfit, using a downhill simplex method (subroutine amoebe, [*Press et. al.*, 1992]). The variables used in this method are t_1, t_2, t_3, and the amplitude a_k of each subevent. Figure 3 shows a representative example of the fit so obtained. From this it can be seen that we are able to determine the beginning and end of the pulse with great detail.

The number of subevents N is fixed by inspection of the stacked P pulse. We here report the duration τ_k of the non-attenuated source time functions. The duration τ_k and moment M_k of the subevents are related through

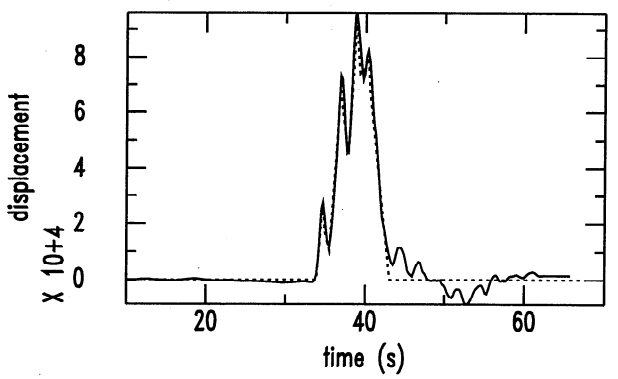

Figure 3. Example of the optimal fit between the stacked trace (solid curve) and the constructed attenuated triangles (dotted curve) for the earthquake of May 3, 1991.

$$M_k = c \times a_k \int d_k(t - t_k)\, dt = \frac{c}{2} \times a_k \times \tau_k, \quad (3)$$

where the constant c is determined by constraining the sum of the moments of the subevents to be equal to the total scalar moment of the recorded event.

3. Results

Table 1 lists the source time parameters determined in this study for each event. Figure 4 shows the measured durations plotted against the corresponding moment of each subevent. As expected, events with large moments tend to have longer durations than events with smaller moments. Since the earthquake duration should be proportional to the linear dimensions of the fault, which, in turn, are proportional to the cube root of the moment, we expect $\log\tau \propto \frac{1}{3}\log M_0$ [*Kanamori and Anderson*, 1975]. From Figure 4 it is clear that there is a discrepancy between this scaling and our data. Despite the large scatter in Figure 4, the discrepancy is statistically significant: regression analysis shows the slope to be equal to 0.16 ± 0.02 rather than $\frac{1}{3}$. The discrepancy is less for the full durations, for which we find a slope of 0.25 ± 0.03. We postpone an investigation of the slope for deep events to a future study. In this study we wish to make a comparison with other studies where a slope of $\frac{1}{3}$ was assumed, and we normalize the durations to conform to a moment of 10^{19} N m by scaling the measured durations by $M_0^{1/3}$. Since there is no significant correlation in our data set between depth and M_0 (correlation coefficient 0.22), the value of the power used in this scaling should not influence a possible dependence on depth.

The durations are plotted versus depth in Figure 5. The values for the total durations (Figure 5a) are in agreement with the earlier studies cited in Section 1. We observe a slight decrease in duration with depth, both for total durations as well as for the subevents durations shown in Figure 5b. The total durations satisfy a least squares fit of

$$t_{\text{tot}} = (9.77 \pm 0.28) - (3.59 \pm 0.82) \times 10^{-3}\, H,$$

and the subevent durations satisfy:

$$t_{\text{sub}} = (9.40 \pm 0.22) - (3.98 \pm 1.22) \times 10^{-3}\, H.$$

where earthquake depth H is in kilometers and t is in seconds. These slopes and intercepts are not significantly different, which indicates a consistent scaling between subevent and total duration. The least squares fit results in an average scaled duration of about 9 s for intermediate-depth earthquakes at 100 km depth to a duration of about 7 s for earthquakes at a depth of 600 km. Understandably, the subevent durations are shifted toward somewhat lower values.

The results of VH are reproduced in Figure 5c. The least squares fitting of scaled durations of these data is;

$$t_{\text{VH}} = (11.79 \pm 0.18) - (9.38 \pm 0.46) \times 10^{-3}\, H.$$

Table 1. Source Time Function Parameters

Date	Time, UT	Latitude	Longitude	Depth, km	N	t_1, s	t_2, s	t_3, s	a_k	M_i, (10^{19} N m)
May 1, 1991	0718:43	62.48	-151.41	118	2	0	5.3	1.1	0.51	0.14
						2.5	6.7	3.4	0.71	0.16
May 3, 1991	0214:14	28.08	139.59	453	4	0	3.1	1.2	2.97	0.091
						1.7	6.6	3.4	7.89	0.39
						4.2	7.3	5.5	9.88	0.31
						5.3	10.5	6.8	9.72	0.51
May 24, 1991	2050:55	-16.51	-70.70	126	1	0	8.0	3.4	2.19	2.12
July 5, 1991	1058:28	47.89	145.80	465	1	0	4.8	2.2	2.85	0.073
Aug. 14, 1991	1253:26	54.39	-169.30	227	2	0	4.1	1.4	0.71	0.034
						1.9	6.0	3.1	1.87	0.086
Aug. 15, 1991	1335:59	-16.06	168.01	189	1	0	6.3	1.6	0.37	0.33
June 16, 1992	0551:03	45.70	142.26	330	1	0	5.0	2.2	3.17	0.11
Sept. 2, 1992	0550:01	-6.05	112.14	636	4	0	2.4	1.4	2.61	0.15
						1.4	5.2	3.5	4.15	0.38
						4.9	7.7	6.6	1.97	0.13
						2.9	10.3	7.9	2.50	0.44
June 8, 1993	2317:41	-31.56	-69.23	124	2	0	3.9	1.3	0.73	0.25
						2.1	5.7	2.6	0.24	0.073
March 14, 1994	2051:24	15.99	-92.43	167	1	0	8.6	3.9	8.76	2.20
May 10, 1994	0636:28	-28.50	-63.10	606	2	0	7.5	3.9	1.06	2.30
						5.0	11.3	8.1	0.13	0.25
June 30, 1994	0923:21	36.33	71.13	253	1	0	4.4	2.4	11.6	0.31
July 21, 1994	1836:31	42.34	132.87	489	2	0	9.5	1.8	60.9	4.54
						3.7	12.3	6.3	96.2	6.46
Aug. 30, 1994	1942:46	-6.97	124.11	604	1	0	5.6	2.6	5.18	0.21
Sept. 28, 1994	1639:51	-5.79	110.35	644	2	0	8.4	2.2	6.39	0.21
						0.2	4.1	4.0	5.17	0.34
Jan. 17, 1995	1654:11	-20.83	-179.24	634	1	0	5.5	1.5	0.33	0.35
March 31, 1995	1401:40	38.21	135.01	366	2	0	2.9	1.0	1.66	0.11
						1.4	5.0	2.2	1.24	0.10
May 5, 1995	2248:04	-18.55	168.78	117	1	0	3.6	0.9	0.17	0.075
May 6, 1995	0159:07	24.99	95.29	147	2	0	5.2	1.2	1.15	0.18
						4.2	8.9	5.1	2.04	0.30
June 24, 1995	0658:06	-3.96	153.93	386	2	0	5.5	1.3	1.18	0.11
						2.9	8.2	5.7	0.75	0.067
June 29, 1995	1224:03	-19.54	169.29	142	1	0	5.4	1.9	2.14	0.91
July 7, 1995	2115:19	33.97	137.13	348	1	0	3.8	1.7	0.46	0.10
Aug. 14, 1995	0437:17	-4.84	151.51	140	1	0	7.7	2.2	4.01	1.40
Aug. 23, 1995	0706:02	18.86	145.22	599	1	0	5.6	3.0	9.35	4.40
Aug. 24, 1995	0155:34	18.90	145.05	588	1	0	2.6	0.9	3.2	0.22
Sept. 16, 1995	0103:36	-6.32	155.21	151	1	0	7.2	3.3	8.09	0.15
Sept. 18, 1995	0656:31	-6.93	128.97	181	1	0	4.0	1.8	0.18	0.12
Oct. 1, 1995	1706:03	29.31	139.04	448	1	0	4.7	2.4	0.32	0.17
Oct. 6, 1995	1139:34	65.17	-148.57	198	2	0	4.3	0.9	0.17	0.11
						1.4	5.1	2.3	0.54	0.29
Oct. 9, 1995	1343:41	-21.47	170.18	105	1	0	5.8	1.9	0.87	0.33
Oct 18, 1995	0930:38	36.43	70.39	223	1	0	6.3	2.7	0.85	0.22
Dec. 25, 1995	0443:24	-6.90	129.15	160	2	0	5.6	2.4	0.46	0.46
						4.0	15.7	9.7	2.09	4.24
Feb. 1, 1996	0718:05	44.86	146.29	180	2	0	5.3	1.5	0.44	0.12
						3.1	7.2	4.7	0.52	0.11
Feb. 22, 1996	1459:09	45.21	148.56	133	1	0	4.3	2.1	1.09	0.36
Feb. 28, 1996	0944:09	1.73	126.10	103	1	0	6.6	2.1	0.61	0.48
March 16, 1996	2204:06	28.98	138.94	477	2	0	6.3	1.5	0.45	0.19
						2.1	7.3	3.9	2.59	0.90
March 17, 1996	1448:56	-14.70	167.30	164	2	0	5.3	2.2	1.9	0.59
						2.2	7.7	4.3	1.9	0.62
May 2, 1996	1334:28	-4.55	154.83	500	1	0	6.8	4.1	0.74	1.00
May 26, 1996	0143:44	-22.19	171.48	108	2	0	4.2	1.5	0.54	0.057
						1.6	7.2	3.0	0.53	0.073
June 9, 1996	0112:16	17.44	145.46	149	1	0	4.5	1.9	0.62	0.71
June 10, 1996	0104:46	-13.48	167.13	196	3	0	11.0	3.3	2.94	0.98
						5.8	9.7	6.9	1.09	0.013
						8.4	12.4	9.6	0.73	0.088

Table 1. (continued)

Date	Time, UT	Latitude	Longitude	Depth, km	N	t_1, s	t_2, s	t_3, s	a_k	M_i, (10^{19} N m)
June 26, 1996	0322:03	27.73	139.75	478	1	0	5.9	1.9	1.28	0.27
July 6, 1996	2136:28	21.97	142.83	252	2	0	8.5	1.4	1.30	0.22
						1.1	5.6	2.4	0.28	0.042
July 15, 1996	1651:22	18.73	145.63	177	1	0	4.6	1.9	0.34	0.28
Aug. 5, 1996	2238:22	-20.69	-178.31	555	3	0	7.2	1.2	1.07	2.80
						1.7	11.3	3.4	2.76	9.60
						4.3	10.4	6.0	0.74	1.60
Aug. 11, 1996	0131:16	-13.40	166.69	100	2	0	5.1	1.6	0.87	0.088
						2.5	6.8	5.5	0.21	0.024
Sept. 24, 1996	1142:18	15.19	-61.44	147	1	0	3.5	0.8	0.14	0.036
Sept. 28, 1996	1410:42	10.04	125.37	235	2	0	4.0	1.5	0.77	0.25
						1.1	5.6	3.5	0.28	0.10

This is a significant departure from the slopes in Figures 5a and 5b. A comparison with Figure 5c shows large durations obtained for several shallow earthquakes in the VH data set. Such long durations are not observed in our data set.

Since most of the data used by VH predate the full growth of the GSN, there is little overlap; however, we used our method to remeasure the duration of the few longest events in the data set of VH for which we could obtain sufficient GSN coverage. We found a mismatch consistent with the difference seen in Figures 5b and 5c whereby the GSN stacks gave far shorter durations. As expected, the scaling with the seismic moment does not influence the conclusion either: scaling the subevent durations with $M_0^{0.16}$ even decreases the magnitude of the slope further to $(1.49 \pm 0.61) \times 10^{-3}$ s/km.

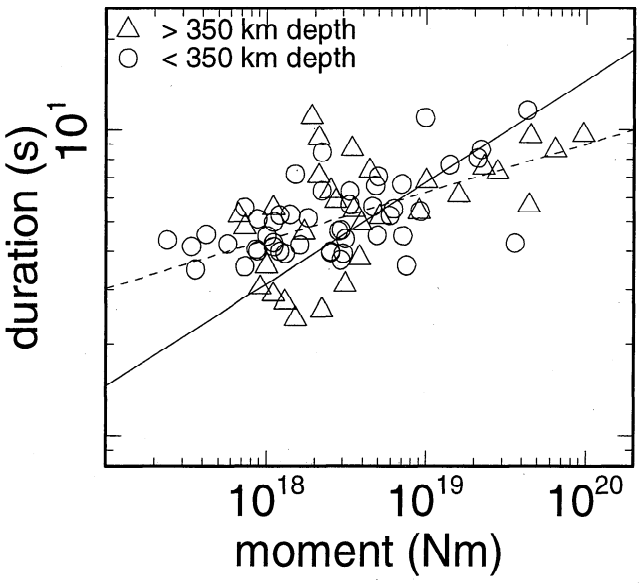

Figure 4. Seismic moment plotted against the measured duration of all the subevents resulting from the source time functions. The solid curve has a slope of $\frac{1}{3}$ showing the expected scaling relationship between duration and the cube root of the moment. The dotted curve has a slope of 0.16, showing the regression line to the data.

4. Discussion and Conclusions

Why do VH observe a much larger dependence of duration on depth? To obtain an answer, we investigated a number of possible causes.

1. It is possible that near source scattered energy is stacked away in global stacks but remained present in the more local (Calnet) stacks of VH. To investigate this possibility, we subdivided our data into segments of different source-station azimuth. Within each segment the ray paths are very close near the source, and scattered energy from within this region should not be attenuated strongly because travel times will not differ greatly. Though the density of the GSN is not large enough to fully mimic a local stack such as used by VH, no significant increase in the stacked coda for such segmented stacks was perceptible, and we do not expect that for an even more local stack an increase will appear. This indicates that the later energy in the P waveform does not originate significantly as near-source scattering.

2. The instruments used by VH are different from the ones used in this study, and it could be that the long durations represent small aftershocks with a high corner frequency that are overshadowed by the more broadband main shock and do not contribute significantly to the broadband GSN records. If this is the case, these aftershocks, contained in the second half of the signal, might be expected to correlate around the globe. By taking the cross-correlation of this second half of the signal, filtered between 0.5 and 2.0 Hz, between all the individual stations, we found that there was no apparent correlation. Globally, aftershocks and later parts of the larger ruptures may not stack well at high frequencies. However, we observed no correlation even between the GSN stations clustered in the United States. This makes this theory highly unlikely.

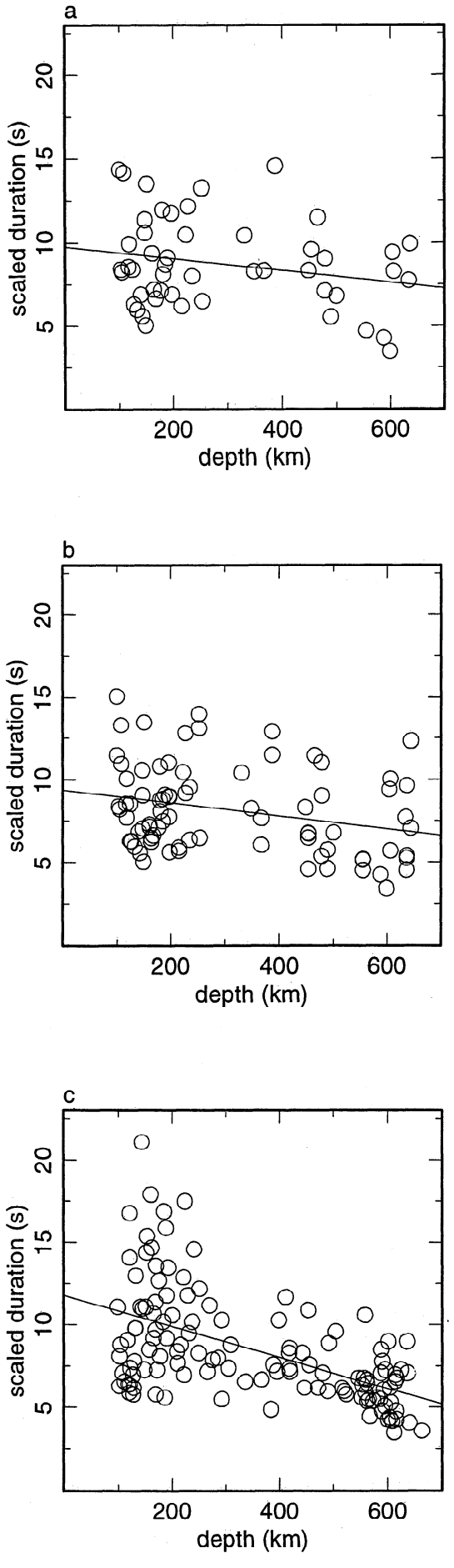

3. Could the long durations be due to anomalously low signal-to-noise ratio? This might be the case if the radiation pattern of the long-duration events is nodal for the Calnet stations. To check this possibility, we recalculated the radiation pattern of these events for the west coast of the United States and confirmed that none of these Calnet recordings were near a node.

4. Finally, we investigated the possibility that the events are at an epicentral distance such that the PcP wave and/or reflections off the D" layer might influence the durations. Whereas near-station scattering will always be incoherent between different seismograms, scattering from objects farther away near the ray path might contribute to a local stack, while being attenuated in a global stack. The region above the core-mantle boundary (CMB) is known to be strongly heterogeneous and would thus be a prime candidate for the origination of scattered waves in the P coda. We plotted the epicentral distance (Δ) versus the duration of the events as measured by VH in Figure 6. The curve in Figure 6 indicates the time delay of the PcP wave with respect to the P wave for a shallow event. It would shift downward by 2.3 s for an earthquake at 600 km depth at 80° (4.7 s at 70°), so it is not very sensitive to earthquake depth and is a good indicator of the time window where energy from the CMB or D" might arrive. It is remarkable that five out of the six events with a duration in excess of 15 s are located to the right of this line, that is, where energy from the CMB itself may arrive. If we lower the threshold to 12.5 s, 11 of the 13 long duration events are possibly influenced by the region around the CMB. This indicates that these measurements may be influenced by reflections from the D"-layer. This is the only reasonable explanation we are able to give.

We conclude that our analysis of GSN data does confirm a small, rather than a large difference in duration between deep and intermediate events. The magnitude of the difference is an indicator for changes in the stress drop. The scaled durations would be expected to satisfy (VH):

$$\frac{\tau}{M_0^{\frac{1}{3}}} \propto \frac{1}{v_s \Delta \sigma^{\frac{1}{3}}}. \tag{4}$$

Knowing the increase of the shear velocity over this depth range to be about 20%, the stress drop would be able to remain constant in order to explain our observed decrease in scaled duration of about 20%. This is consistent with the observed stress drops, which are

Figure 5. Moment scaled durations plotted versus depth. (a) The total durations of the events used in our study measured from global stacks of Global Seismograph Network seismograms. The least squares fit is shown by the solid curve. (b) Similarly, the plot of the durations of all the subevents. (c) The results of VH, measured from local stacks of Calnet stations.

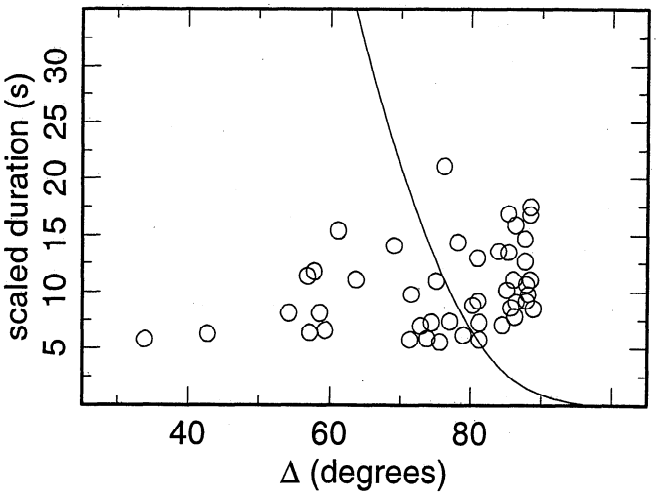

Figure 6. Average epicentral distance for the Calnet stations used by VH versus scaled duration. The curve represents the time difference between the arrivals of the PcP- and P wave. The measured durations plotted near or on the right side of the curve can be affected by reflections from the D"-layer.

mostly constant with depth [*Houston and Williams*, 1991; *Fukao and Kikuchi*, 1987; *Wyss and Molnar*, 1972] or may show a slight increase with increasing depth [*Frohlich*, 1989]. This implies that in this sense deep earthquakes are comparable to shallow ones.

Acknowledgments.
A. Bos would like to thank the department of Geosciences, Princeton University, for support during a summer stay.

References

Azimi, S.H.A., A.V. Kalinin, V.V. Kalinin, and B.L. Pivovarov, , Impulse and transient characteristics of media with linear and quadratic absorption laws, *Earth Phys.*, *2*, 42-54, 1968.

Chung, W., and H. Kanamori, Variation of seismic source parameters and stress drops within a descending slab and its implications in plate mechanics, *Phys. Earth Planet. Inter.*, *23*, 134-159, 1980.

Ekström, G., and E.R. Engdahl, Earthquake source parameters and stress distribution in the Adak Island Region of the central Aleutian Islands, Alaska, *J. Geophys. Res.*, *94*, 15,499-15,519, 1989.

Frohlich, C., The nature of deep-focus earthquakes, *Annu. Rev. Earth Planet. Sci.*, *17*, 227-254, 1989.

Fukao, Y., and M. Kikuchi, Source retrieval for mantle earthquakes by iterative deconvolution of long-period P waves, *Tectonophysics*, *144*, 249-269, 1987.

Houston, H., and Q. Williams, Fast rise times and the physical mechanism of deep earthquakes, *Nature*, *352*, 520-522, 1991.

Kanamori, H., and D.L. Anderson, Theoretical basis of some empirical relations in seismology, *Bull. Seism. Soc. Am.*, *65*, 1073-1095, 1975.

Kanamori, H., and J.W. Given, Use of long-period surface waves for rapid determination of earthquake-source parameters, *Phys. Earth Planet. Inter.*, *27*, 8-31, 1981.

Press, W.H., B.P. Flannery, S.A. Teukolsky, W.T. Vetterling, Numerical recipes, Cambridge Univ. Press, 963 pp., 1992.

VanDecar, J.C., and R.S. Crosson, Determination of teleseismic relative phase arrival times using multi-channel cross-correlation and least squares, *Bull. Seismol. Soc. Am.*, , *80*, 150-159, 1990.

Vidale, J.E., and H. Houston, The depth dependence of earthquake duration and implications for rupture mechanism, *Nature*, *365*, 45-47, 1993.

Wyss, M., and P. Molnar, Source parameters of intermediate and deep-focus earthquakes in the Tonga arc, *Phys. Earth Planet. Inter.*, *6*, 279-292, 1972.

A. G. Bos, Faculteit Aardwetenschappen, Afdeling Geofysica P.O. Box 80.021, 3508 TA Utrecht, Netherlands. (e-mail: bos@geof.ruu.nl)

H. Houston and J. E. Vidale, Earth and Space Sciences Department, University of California, Los Angeles, CA 90095-1567

G. Nolet and A. Rubin, Department of Geosciences, Princeton University, Princeton NJ 08544

(Received August 8, 1997; revised January 30, 1998; accepted April 17, 1998.)